NORWEGIAN JOURNAL OF GEOLOGY
https://dx.doi.org/10.17850/njg105-3-3

GEOLOGICAL SOCIETY OF NORWAY

Rhomb-porphyry eruption dynamics in the Oslo Rift recorded in pyroclastic fissure conduits

Jack W. Whattam[1], Dougal A. Jerram[2,3], Ivar Midtkandal[1], Bjørgunn Heggem Dalslåen[1], Sara Callegaro[1,4] & Henrik H. Svensen[1,2]

[1]*Dept. of Geosciences, University of Oslo, Norway.*
[2]*Njord Centre, Dept. of Geosciences, University of Oslo, Norway.*
[3]*DougalEARTH Ltd., Solihull, UK.*
[4]*Dept. of Biological, Geological, and Environmental Sciences, University of Bologna, Italy.*

E-mail corresponding author (Jack Whattam) jackww@uio.no

Keywords:
- *Rhomb-porphyry*
- *Oslo Rift*
- *Conduit*
- *Volcanism*
- *Eruption dynamics*

Received:
6. November 2024

Accepted:
1. October 2025

Published online:
10. Desember 2025

Highlights:
- *First field-evidence of rhomb-porphyry fissure conduits in the Oslo Rift.*
- *Outcrops reveal complex eruption dynamics, with explosive component.*
- *Rhomb-porphyry spatter and lava-tops show similar characteristics.*
- *Reassessment of rhomb-porphyry eruption styles in the Oslo Rift.*

Dike-fed fissure vent complexes are commonly linked to basaltic eruptions but are also proposed for some intermediate to silicic eruptions in Large Igneous Provinces (LIPs) and continental rifts. Direct evidence of these complexes is scarce however, and our understanding of the associated eruptive processes remains limited. Basaltic and trachy-andesite (i.e., rhomb- or rectangle-porphyry: RP) eruptions across the Oslo Rift (part of the Skagerrak-Centered LIP) are assumed to have erupted from similar dike-fed fissures, although no direct evidence of eruptive vents has been identified. We present observations illustrating the presence of a shallow (<80 m paleo-depth) RP fissure conduit in the central Oslo Rift recording explosive eruptive activity. Previous workers interpreted these outcrops as a partially preserved lava, suggesting the basaltic unit was cross-cutting due to deposition in an erosional depression. Our studies of outcrops, hand-samples, and thin-sections illustrate three primary textural zones: 1) a core zone with ductile deformation and moderate fragmentation; 2) a heavily-fragmented ash-rich margin zone with inclusions of both rhomb-porphyry and host rock (basalt); and 3) an edge zone variably characterised by un-brecciated rock or brecciated rock with ash-filled fractures. Lateral textural gradations (over 1–3 m width) from core to brecciated host-rock and substantial overall width (~40 to <<100 m), are consistent with a near-surface (<80 m) paleo-depth, whilst heavily fragmented margins suggest mild to moderate explosive activity towards the end of the associated eruptive episode. An exposure of a slabby- to rubbly-pahoehoe RP8 flow top with mingled and overlying pyroclastic (i.e., ash and lapilli) components additionally highlights explosive processes operating in the late stages of older RP eruptions. Our observations provide the first direct evidence of elongate eruptive-conduits (i.e., fissure-conduits) in the Oslo Rift, but textural characteristics illustrate that at least some rhomb-porphyry eruptions were punctuated by episodes of moderately explosive activity during waning eruptive activity.

Whattam, J.W., Jerram, D.A., Midtkandal, I., Dalsåen, B.H., Callegaro, S. & Svensen, H.H. 2025: Rhomb-porphyry eruption dynamics in the Oslo Rift recorded in pyroclastic fissure conduits. *Norwegian Journal of Geology 105*, 202512. https://dx.doi.org/10.17850/njg105-3-3

Introduction

Pyroclastic-dikes, diatremes, and tuffisites are shallow (<1 km depth) to near-surface magmatic feeder systems (e.g., Delaney & Pollard, 1981; Heiken et al., 1988; Tuffen et al., 2003; Lefebvre et al., 2012; Re et al., 2016; Unwin et al., 2023), often directly associated with an eruption. Studying these shallow feeder systems and any associated or analogous eruptive products may elucidate processes associated with shallow magmatic transport and eruption (Lefebvre et al., 2012). Observations of pyroclastic, spatter-rich vent complexes and dikes within flood basalt provinces have highlighted the occurrence of vigorous explosive pulses in dominantly effusive settings. In addition, a reappraisal of hybrid (i.e., effusive and explosive) silicic systems suggests that effusive silicic activity is a product of prior inconduit fragmentation and sintering (Wadsworth et al., 2022). Documented occurrences of shallow pyroclastic magmatic feeders span a range of compositions (basaltic to rhyolitic: e.g., Kano, 2002; Tuffen et al., 2003; Díaz-Bravo & Morán-Zenteno, 2011; Lefebvre et al., 2012; Re et al., 2016), dimensions (centimetres to >100 m: e.g., Keating et al., 2008; Geshi et al., 2010; Vezzoli & Corazzato ,2016), and locations (typically extra- or intra-caldera or volcanic rift settings: e.g., Aguirre-Díaz & Labarthe-Hernández, 2003; Galindo & Gudmundsson, 2012; Unwin et al., 2021, 2023). However, due to limited exposure in young volcanic provinces, or loss through erosion in ancient provinces, these systems remain poorly understood in many volcanic provinces.

Although the Oslo Rift (Fig. 1A) has been extensively studied (e.g., Sæther, 1962; Naterstad, 1978; Oftedahl, 1978a, b; Neumann et al., 2006; Larsen et al., 2008; Neumann, 2019; Corfu & Larsen, 2020; Rämö et al., 2022), there is still much to learn. New opportunities (e.g., borehole cores and road-cuts from major road-construction projects; e.g., Dalslåen et al., 2024), have prompted renewed interest in the Oslo Rift among researchers. Additionally, emplacement models of volcanic and subvolcanic systems (e.g., Branney & Kokelaar, 2002; Brown & Branney, 2004, 2013; Ross et al., 2005; Branney et al., 2008; Burchardt, 2008; Galland et al., 2009, 2019; Manville et al., 2009; Tuffen et al., 2013; Brown et al., 2014; Sohn & Sohn, 2019; Wadsworth et al., 2022) have changed markedly since much of the classical geological mapping, stratigraphy, and description of the Oslo Rift were undertaken (e.g., Sæther, 1946; Oftedahl, 1959, 1978a; Naterstad, 1978). Notably, the eruptive and depositional processes associated with the rhomb- and rectangle-porphyry (RP) lavas across the Oslo Rift are particularly enigmatic and have received limited modern study. The rhomb-porphyry lavas have long been envisaged as originating from monogenetic and polygenetic fissure systems, evidenced by the many NW–SE-oriented dikes found inside and outside of the main rift (Oftedahl, 1978b; Larsen et al., 2008). However, clear evidence of a feeder dike, either through direct connection with its associated lava flow (Sundvoll et al., 1990) or through clear textural evidence, has not been documented. Furthermore, whilst fissure-type vents are common in LIPs and volcanic rift systems (White et al., 2009), they are not characterised solely by effusive activity (Brown et al., 2014) and are not limited to eruptions of basaltic compositions (Bryan et al., 2000; Aguirre-Díaz & Labarthe-Hernández, 2003; Navarrete et al., 2021). Here, we re-examine and provide the first detailed descriptions of RP outcrops in the central Oslo Rift (Alnsjø: Fig. 1) which have been briefly mentioned in previous research (Holtedahl, 1943; Sæther, 1962; Naterstad, 1978). Whilst Naterstad (1978) ascribed the occurrence of these RP outcrops to partial preservation of a channel-filling lava, we present evidence illustrating an alternative interpretation that these outcrops represent a shallow (ca. <80 m) pyroclastic dike that likely fed one of the youngest RP eruptions in the Oslo Rift.

Geologic Setting

Tectono-magmatic evolution in the Oslo rift, active from ca. 300 to 265 Ma (Corfu & Larsen, 2020), is generally divided into six stages: 1) a proto-rift stage comprising marine to terrestrial sedimentation, and magmatic intrusions (sills and dikes); 2) an initial volcanic stage comprising large-volume effusive basaltic eruptions; 3) a main-rift stage dominated by voluminous eruptions of rhomb-porphyry (trachy-andesite) lavas; 4) a main- to late-rift transitional stage comprising eruption of mafic to silicic compositions from central vent complexes; 5) a late-rift stage with emplacement of silicic batholiths; and 6) a termination stage characterised by dike swarm emplacement (Olaussen et al., 1994; Sundvoll & Larsen, 1994; Larsen et al., 2008). The exact nature of later stages (stages 4–6) is comparatively less understood as substantial post-rift erosion has removed most of the associated surface deposits. Large-scale basaltic volcanism was concentrated in the early rift stage between ca. 302 and 298 Ma (Torsvik et al., 2008) whereas rhomb-porphyry volcanism appears to have occurred throughout most of the rifts history: The earliest RP lava (denoted RP1) is dated at ca. 299 Ma, and middle to late RP lavas (RP8 and RP11) are dated at ca. 285 and 280 Ma, respectively. An RP dike in the central rift gives the youngest known age of any magmatic rock in the Oslo Rift at ca. 265 Ma (Corfu & Larsen, 2020). Silicic volcanism began at ca. 280 Ma, approximately contemporaneous with late-stage mafic (basaltic lava packages B3 and B4) and RP (RP11 to RP14 or RP15) volcanism (Corfu & Larsen, 2020; Larsen et al., 2008).

The primary study area (Alnsjø, Fig. 1B) is located north-east of Oslo, at the southern edge of the Nittedal caldera within the Krokskogen transfer zone (Naterstad, 1978; Larsen et al., 2008), and is suggested to host the youngest volcanic and sedimentary deposits in the rift (Sæther, 1946; Naterstad, 1978). Several basaltic lavas (either B3 or B4 stage: Oftedahl, 1978b; Naterstad, 1978) are observed as the basal units of the area (Whattam et al., 2024). These are overlain by a succession of basaltic tuff breccias, variably welded ignimbrites, and sediments with intercalated volcanic deposits (Whattam et al., 2024). Subsequent deformation has formed a synclinal structure, previously described as a boat-shaped syncline (Naterstad, 1978), with steeply dipping limbs parallel to the east-west axis, and gently dipping limbs parallel to the north-south axis. Although previously suggested to be a caldera infill succession, recent work (Whattam et al., 2024) has shown there is no evidence for this. Instead, the deposition occurred in a rift valley setting, later preserved as a subsided caldera block. A second, complimentary study area (Avtjerna, Fig. 1A), is located at the western end of the Krokskogen transfer zone, approximately 25 km west of Alnsjø. This area sits within the Krokskogen lava plateau, with an areal extent of ~400 km^2 and approximately 900 m of preserved stratigraphy, of which roughly 80% is composed of rhomb-porphyry lavas (Larsen et al., 2008). Middle- to late-stage RP lavas (RP7–RP9) are exposed in Avtjerna, with a basaltic lava package (B2) and minor sediments overlying RP9 approximately 500 m to the northwest. Farther northwest (~15 km) the succession can be followed into silicic ignimbrites. However, the stratigraphic relationship is complicated by faulting, likely related to caldera collapse eruptions associated with the ignimbrites.

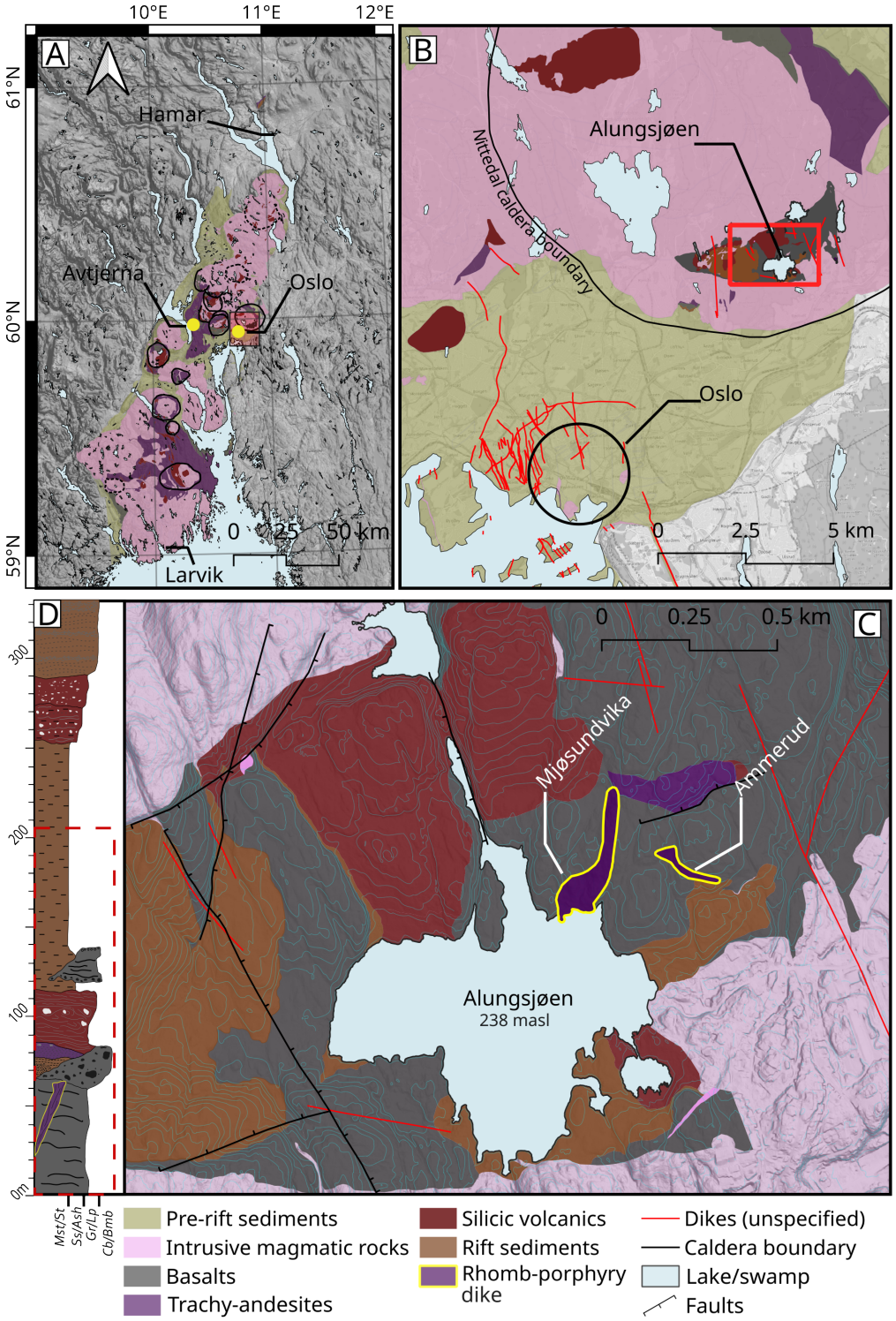

Figure 1. (A) Simplified geological maps of the Oslo Rift. (B) The central rift region around Oslo. (C) Geology of the study area (based on the geological map of Whattam et al., 2024) highlighting the two localities of the studied rhomb-porphyry dikes at Mjøsundvika and Ammerud. (D) A simplified stratigraphic column highlights the location of the dike within the entire Alnsjø stratigraphy (modified from Whattam et al., 2024). The red dashed box indicates the stratigraphy exposed in the map area shown in C. Abbreviations in D are: Mst/St - mud/silt; Ss/Ash - sand/ash; Gr/Lp - gravel/lapilli; Cb/Bmb - Cobble/block-bomb.

Methods

Field mapping was undertaken in the Alnsjø area during the summers of 2021–2023. Exposure across the area is generally limited, and outcrops are heavily weathered in many places. As a result, identifying lithofacies and detailed textural characteristics requires a combination of careful outcrop observation, cut and semi-polished hand-samples, and thin-sections. Samples and photographs of the main outcrops and textural variants were collected to facilitate multi-scale analysis of core, margin, and wall-rock units. Thin-sections were prepared from the best hand specimen from each zone and used for micro-textural study. Hand-samples were cut, roughly polished with a 400 μm diamond lapping plate, and scanned with a flat-bed photo scanner. Thin-sections were scanned in plane-polarised and cross-polarised light using a Zeiss AxioScan polarising thin-section scanner at 20x magnification and further examined using a standard petrographic microscope. Field observation of the rhomb-porphyry lavas in Avtjerna was undertaken during two day trips in the summer of 2024. The fieldwork included identification of major clast components, textures, and obtaining images for later analysis.

Results

As stated, the key facies and facies associations have been recorded at the outcrop scale and through sampling for polished hand samples and thin-sections where appropriate, to help resolve the complex facies relationships. Qualitative and quantitative textural and petrological characteristics from macro to micro scale are described below and are summarised in Table 1.

Field relationships and outcrop characteristics

The stratigraphic succession preserved in Alnsjø (Fig. 1D) comprises basaltic lava flows, pyroclastic basaltic deposits, trachy-andesite to rhyolitic ash-tuffs, silicic ignimbrites, and several sedimentary units. Simple a'a-type basaltic lavas comprise the base of the succession; the rhomb-porphyry dike cuts the basal basaltic unit in eastern Alnsjø. The basal lava series is variably overlain by pyroclastic basaltic deposits in the west and sandstone, conglomerate, and a trachy-andesite ash-tuff in the east. An erosional unconformity separates these units from overlying silicic ignimbrites which in turn are overlain by mudstone (with an interbedded basaltic flow), a moderately welded ignimbrite, and a volcaniclastic conglomerate.

Two mapped areas of RP (Mjøsundvika and Ammerud; Figs. 1C & 2) show clear cross-cutting relationships to the adjacent units. The contacts for the Mjøsundvika and Ammerud outcrops are oriented approximately north-south and northwest-southeast. They are vertical (ca. 90°) and sub-vertical (ca. 70°), and cross-cut horizontal and sub-horizontal (<10°) host-rocks, respectively. A transition from phenocryst-rich deformed and fragmented core, through a complex heavily-fragmented margin zone, to undeformed host-rock (basalt) is preserved in the Mjøsundvika exposure (Figs. 1B & 2B). In contrast, the Ammerud exposure (Fig. 2B) has similarly deformed and fragmented core material but is juxtaposed with a planar bedded sandstone host-rock with only a thin (<30 cm), heavily eroded margin zone. Given the greater preservation and exposure of the Mjøsundvika outcrops we focus on these. However, the characteristics of the margin zone in the Ammerud locality provide an important comparison. Outcrops exhibiting both margins have not been found. However, in the Mjøsundvika locality a distinct 3–5 m-wide, north-south oriented erosional depression with RP exposed along the east and basalt along the west is indicative of the western margin.

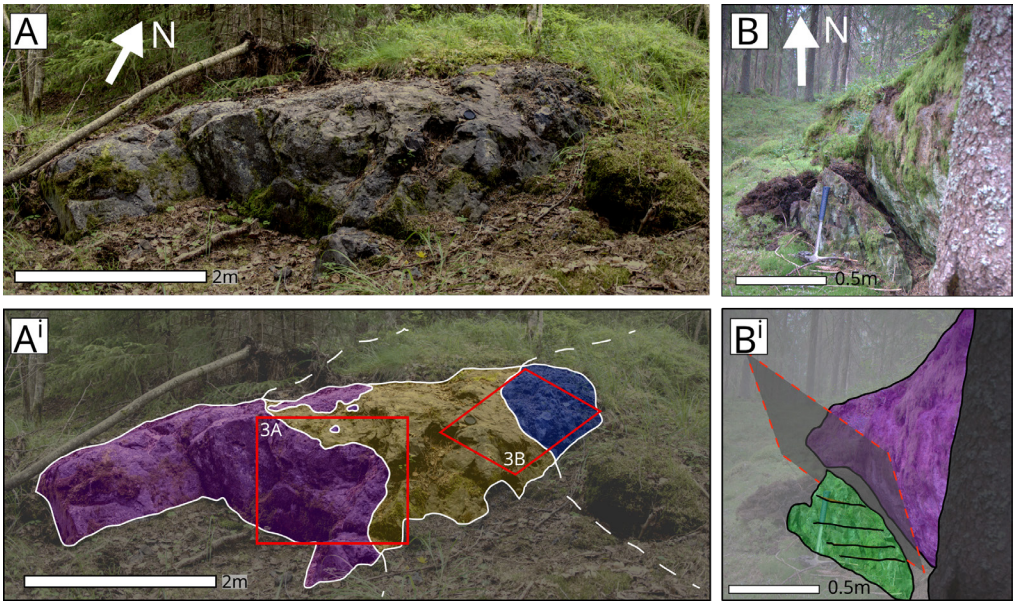

Figure 2. Outcrop images and interpretations of two key outcrops: Mjøsundvika (A and A^i) and Ammerud (B and B^i). Dike zones (purple: dike core; yellow: margin) and host rock (blue: basalt; green: sandstone). Red boxes in Ai are areas covered in Fig. 3A, B. Dashed white lines in Ai show approximate covered continuation of zones. Contact plane is shown in Bi.

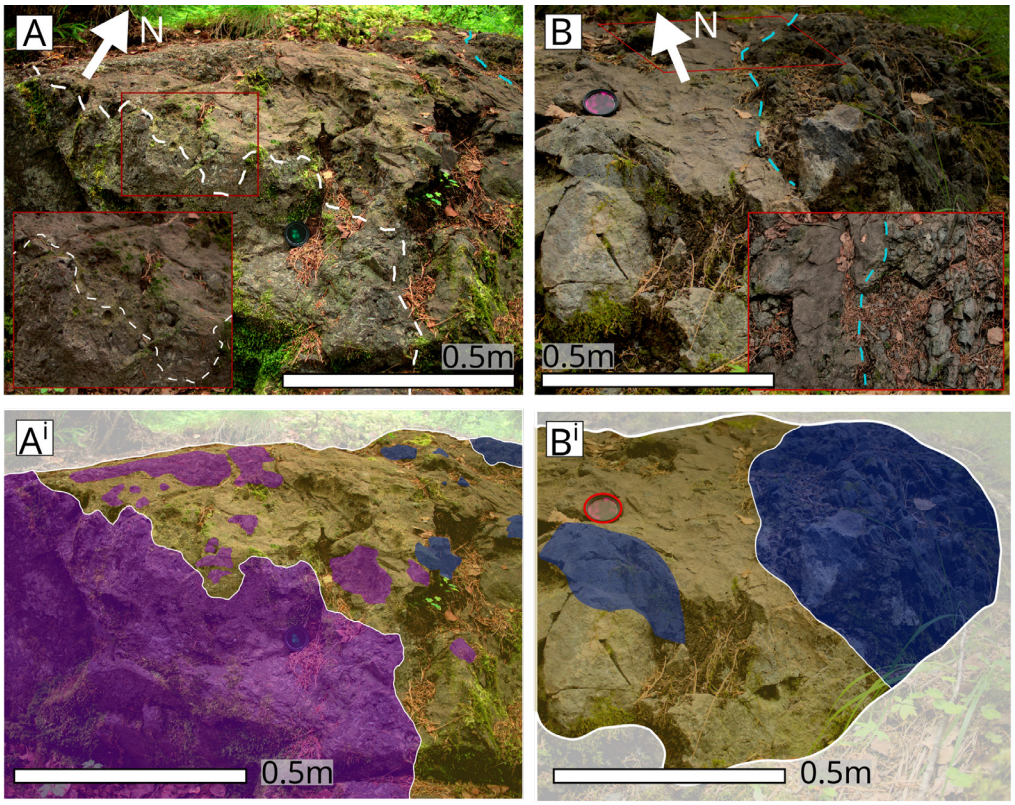

Figure 3. Detailed images from the Mjøsundvika outcrop (Fig. 2A) showing a transition from coherent RP to a pyroclastic margin zone (A and A^i) and the contact between the margin and edge zones (B and Bi). The inset images in A and B are enlargements showing greater detail of the boundaries between coherent RP and RP rich pyroclastic margin, and margin to edge transition, respectively. White and blue dashed lines delineate core-margin and margin-edge boundaries in the outcrop. In the margin zone, clasts are initially dominated by RP, with a rapid marked change to basalt toward the contact with the wall-rock (to left of A^i).

Host-rock units

In Mjøsundvika, the dike cuts through an extensive, mixed basaltic lava unit consisting of pahoehoe and a'a type. Outcrops of the basalt have limited vertical continuity (ca. <5 m) and the total thickness is unknown as no base has been observed. The deposit varies between coherent (i.e., lacking clastic textures) and clastogenic forms. Coherent portions are porphyritic and poorly- to moderately-vesicular, with plagioclase phenocrysts ranging from <0.5 mm to ~6 mm. Clastogenic portions are composed of poorly vesicular, slightly to moderately porphyritic clasts, with subordinate scoria and angular to sub-angular breccia, and rare moderately vesicular basalt, in an ash-sized groundmass. Porphyritic clasts in clastogenic portions have rounded to irregular shapes, slightly to moderately elongated forms, whereas angular clasts are more equant. The groundmass is composed of fine-lapilli sized basaltic fragments and glassy to ash-sized material. A sub-horizontal orientation (at least locally) of the basalt is suggested by sub-horizontal to horizontally oriented vesicles and a vertical gradation in vesicle

Table 1. Main features of rhomb-porphyry dike and lava crusts

	Width (m)	Thickness (m)	Textural composition	Clasts	Groundmass	Vesicles	Notes
Core	25–60	n.a.	Moderate to heavily welded, clast dominated lapilli tuff.	Amoeboidal/fluidal shapes, ~3–30 cm size, abundant 2–30 mm unbroken plagioclase phenocrysts, rare fine (<1 cm) country rock clasts.	Devitrified ash/glass, sparse to moderately abundant phenocrysts of mostly fragmented plagioclase.	Abundant small (<1 mm) vesicles in three populations: highly elongate/flattened; slightly deformed and often coalescing; and round (undeformed) isolated vesicles.	Local variations in width common.
Margin	0.75–3	n.a.	Moderately to poorly welded, ash rich lapilli tuff.	Lapilli to bomb sized clasts (typically lapilli), of RP and host rock. RP clasts typically have amoeboidal shapes whereas host rock clasts are blocky or angular.	Fine ash (<0.25 mm) with some medium ash (<0.5 mm). Abundant phenocryst fragments.	Poorly vesicular (<5%) with micro-vesicles (<0.05 mm)	Not always present, margin between core and host rock can be sharp.
Edge	<1	n.a.	Brecciated in-situ host rock, apparent gradation from un-brecciated to finely brecciated towards margin zone.	Angular to sub-angular, fine (<1 cm) to coarse (>0.5 m) breccia.	Fine to medium interstitial ash filling fractures. Micro-phenocrysts and phenocryst fragments (<0.5 mm size) in the interstitial ash.	No volcanic vesicles observed but void spaces present in breccia (may be due to later erosion).	Degree of brecciation is influenced by host rock lithology, duration of conduit activity, and type of volcanic activity.
Spatter	n.a.	~10	Pervasive low- to moderate grade welding with sintering necks and clast suturing. Subtle diffuse stratification in outcrop.	Sub-angular to amoeboidal coarse lapilli (<64 mm) with occasional bomb-sized clasts. Occur as moderately low-vesicularity, crystal-rich and crystal-poor, vesicle-rich populations. 'ghost pyroclasts'.	Fine to medium ash. Typically volumetrically minor.	Moderately abundant fine collapsed and deformed vesicles.	
Mingled crust	n.a.	1–2	Mixture of blocks and folded or stretched slabs with rounded and irregularly shaped lapilli and interstitial ash.	Clasts ~5–15 cm, moderately vesicular, blocky, angular to sub-angular, or sub-rounded irregular.	Fine to medium ash, sparse phenocrysts, some coarse ash to very fine lapilli.	Sparse fine collapsed and deformed vesicles.	

abundance in an exposure 15 m east of the Mjøsundvika outcrops. Field mapping evidence suggests this unit occupies the same stratigraphic level as the basalts comprising the base of succession in western Alnsjø. In Ammerud, the host unit is a dominantly planar stratified sandstone with thin to very-thin (ca. 5–15 cm) alternating beds comprising fine and medium to coarse sand. This unit has limited areal preservation, comprising one continuous outcrop ca. 4 x 30 m (in size). Sparse, subtle ripples and cross-stratification are observed, indicating a broadly westwards transport direction. A small area of fine pebbly-sand to fine conglomerate appears at the top of some outcrops, suggesting an upward- coarsening sequence. Grains are angular to sub-angular and are composed of fragments of basalt, plagioclase, and quartz.

RP dike

Core region

The core of the RP dike (Fig. 4A, A^1, A^2) comprises moderately- to heavily welded, poorly sorted, lapilli tuff to massive agglomerate facies (sensu Branney & Kokelaar, 2002) with abundant plagioclase

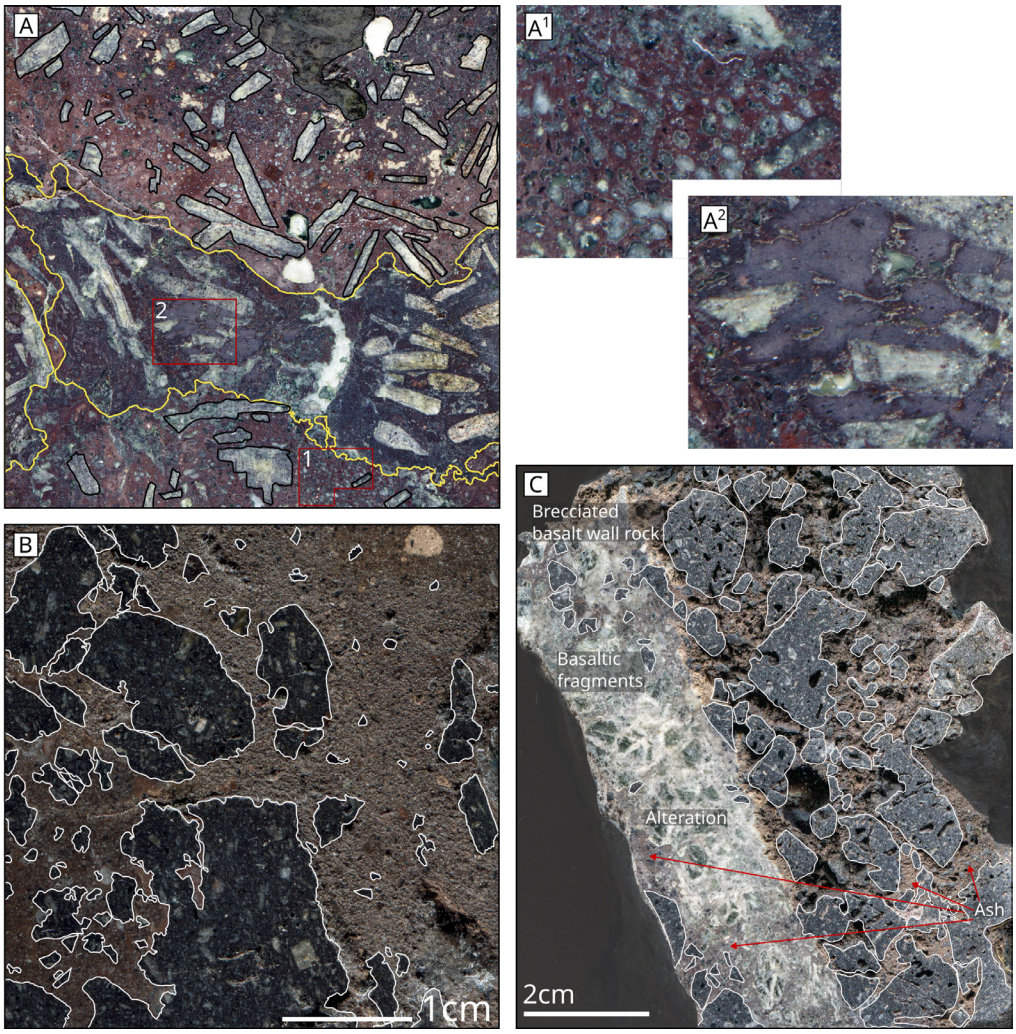

Figure 4. Hand-sample scans showing textural details of core and margin zones in Mjøsundvika, highlighting pyroclastic textures in the core material, ash and co-mingled basalt in the margin, and wall-rock brecciation. Clasts in the dike core (yellow outlines in A) have highly irregular margins, fewer vesicles, approximately consistent phenocryst orientations, and a generally darker colour than the surrounding groundmass. Vesicularity in the groundmass ranges from low to very-high (A1) and some clasts show highly sheared vesicles (A2). Pyroclastic dike margin (B) comprising brecciated basalt in an ash-rich matrix. C) shows the transition into the edge zone with in situ brecciated basalt, with ash filling interstitial space in the breccia, and a larger ash-filled fracture with significant alteration.

phenocrysts. Clast sizes range from several centimetres to several tens of centimetres and have highly irregular margins, with abundant phenocrysts. Phenocrysts occur both as intact and broken varieties and range from ca. 2 to 30 mm in length. Except for some triangular fragments, they primarily have rectangular forms. Broken phenocrysts occur both within clasts and within the groundmass but are more common in the groundmass. The groundmass consists of devitrified glass and very-fine ash, with zones of abundant small (ca. <1 mm) round to heavily elongated vesicles, now filled with secondary minerals (Figs. 4A[1] & 5C, D, F) and moderately-abundant to abundant microlites (Fig. 5F). Sparse blocky mafic clasts are also observed in the groundmass (Fig. 5B–C).

Margin region

An ash-rich zone with a mixture of RP and basalt clasts is here termed the "margin zone" (Fig. 4B). Notably, this zone was not observed around the Ammerud outcrops. Where exposed in the Mjøsundvika outcrops it was substantially wider at the western margin (~3 m wide) than at the eastern margin (~0.75–1 m wide). The zone comprises poorly- to moderately sorted lapilli tuff, with very-fine to medium (and some coarse) ash, with lapilli- to bomb-sized RP and basalt clasts (typically lapilli sized; Fig. 5A, B). Calcite alteration is prevalent in some samples and includes alteration of both plagioclase phenocrysts and groundmass (Fig. 5B). Micro-vesicularity in the ash is visible in thin-section but is low (~<5%). At macro-scale, RP clasts generally have more irregular to amoeboidal shapes, whereas basalt clasts have blockier to rounded forms. However, at the micro-scale, irregular margins are present in basalt clasts as well (Fig. 5A, B). Clasts show lateral grading both in size and abundance. RP clasts are larger and more abundant proximal to the core zone, whilst the opposite is true for basalt clasts. No clast or phenocryst alignments, deformation, welding, or fiamme are distinguishable in the margin zone.

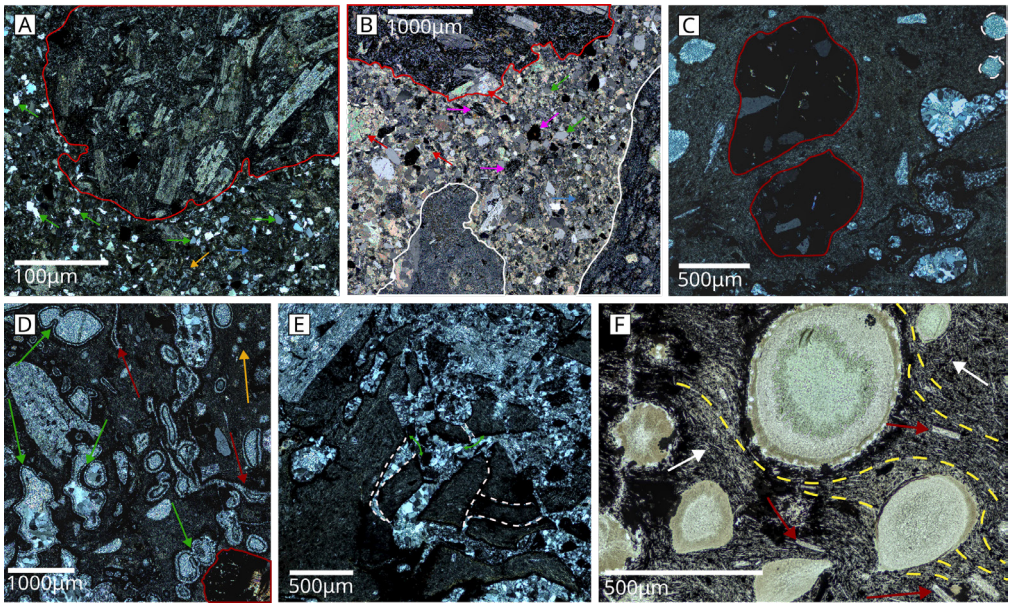

Figure 5. Photomicrographs from the Mjøsundvika outcrop showing micro-textures from the margin (A), margin proximal to edge (B), and core (C–F) zones. A and B show basaltic (red outlines) and RP (white outlines) clasts in an ash groundmass with arrows indicating quartz (green), feldspar (orange), basalt fragments (pink), and devitrified glass (blue). Red arrows in B highlight calcite alteration of plagioclase phenocrysts and devitrified glassy groundmass. Sparse, blocky mafic clasts (red outlines in C and D) are also present in the core. The core zone shows variable deformation styles: Vesicles in D) show ductile deformation and coalescence (green arrows), collapse and shear (red arrows), and undeformed micro-vesicles (yellow arrow); Glassy material in E) exhibits brittle fracture (white dashed lines, green arrows indicate movement). F) Micro-phenocrysts (red arrows) and microlites (white arrows) are abundant in the glassy material with fabrics wrapping around vesicles (yellow dashed lines).

Edge region

The edge (Fig. 4C) is here defined as the area where the host rock is brecciated but not significantly disaggregated (i.e., appears to be in situ). In Ammerud, the dike cross-cuts a sub-horizontal planar-stratified sandstone with no obvious deformation or fracturing of the sandstone. However, due to the limited exposure in Ammerud, very coarse brecciation (>0.5 m blocks) would not be distinguishable. In Mjøsundvika, the dike cross-cuts a sub-horizontal basaltic lava with substantial deformation and brecciation. A gradational transition from margin to edge to undeformed basalt occurs over ~1 m in the Mjøsundvika outcrops. Within 20–30 cm of the margin zone the basalt is heavily brecciated but appears to be in situ (i.e., has been fractured in place), with ash filling all the fractures. At 30–100 cm from the margin, the basalt appears progressively less fractured, although no continuous outcrops have been found to fully expose this transition.

RP lava crusts

Recent civil works west of Oslo (Avtjerna: Fig. 1) have exposed an area of RP7 and RP8 with complex spatter or agglutinated pyroclastic deposits (RP7) and complex lava crust (RP8). In addition, both RP7 and RP8 are overlain by discontinuous ash layers which are also seen in cores and other outcrops in the Avtjerna area (B. Dalslåen pers. comm., 2024).

RP7 spatter breccia

The deposit has a maximum observed thickness of 10 m, although significant lateral thickness variations occur. It is predominantly characterised by ash and sub-rounded to elongate and deformed coarse lapilli (<64 mm), with some larger bomb-sized clasts. Although the deposit appears chaotic in outcrop, stratigraphic sampling of the section reveals variations in dominant grain size (ranging from coarse lapilli and bomb dominated to fine lapilli dominated) suggesting the presence of subtle, diffuse stratification. Clasts comprise both moderately low-vesicularity, crystal-rich RP, and crystal-poor vesicle-rich varieties, although clasts span a full range from dense to highly vesicular, with variable vesicle sphericity (Fig. 6A–C). Lapilli and coarse ash also show a variety of clast shapes, ranging from sub-angular to irregular, amoeboidal forms (Fig. 6C), with fluidal ‘tongues’ (Fig. 6D) where clasts and ash have deformed together. In hand-sample and thin-section, collapsed and deformed vesicles (Fig. 6B), sintering necks (Fig. 6G), and clast suturing (Fig. 6H) are commonly observed, indicating pervasive welding and agglutination. Some samples show only faint remnant clast boundaries (Fig. 6H: e.g., ‘ghost pyroclasts’ sensu Re et al., 2016) resulting from intense welding.

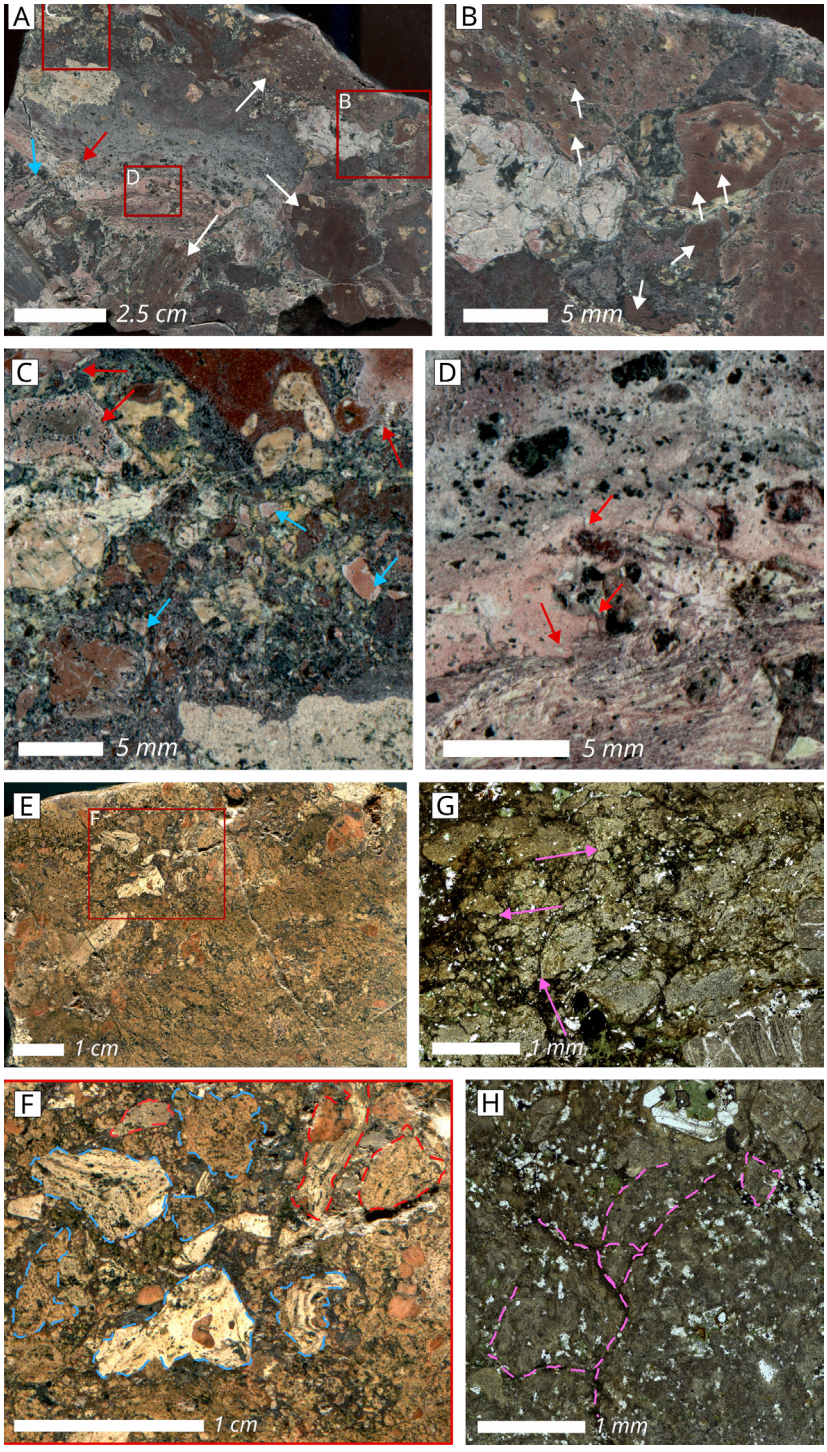

Figure 6. Hand sample scans (AF) B, C, D and F are zoomed images of A and E, respectively, of the RP7 spatter breccia. Arrows in A–D highlight clasts with contrasting vesicle and phenocryst populations (white), and both brittle (blue) and ductile to fluidal (red) features in a single lapilli-rich sample from the RP7 spatter. Vesicles in lapilli (white arrows in B) range from spherical and sub-spherical to highly flattened, indicating distinct vesiculation and deformation histories for individual clasts in the sample. The groundmass (C) comprises fine to coarse ash and crystal fragments with both angular (blue arrows) and rounded to fluidal (red arrows) forms. Ductile deformation and textures suggestive of minor flow (red arrows in D) are present at mm to sub-mm scale. Fine-grained portions of the RP7 spatter show higher degrees of alteration (E–F) but are broadly similar, comprising clasts with both angular (red outlines) and rounded to fluidal (blue outlines) forms, fine to coarse ash (more abundant than in A), and phenocryst fragments. Photo-micrographs (G & H) of the groundmass components of Av–A (cut from same sample as E) highlight agglutination (pink arrows in G) and suturing (pink outlines in H: e.g., welding and deformation under compression: Giachetti et al., (2021) of coarse ash (<2 mm) to fine-lapilli.

RP8 lava crusts

RP8 exhibits a ca. 1–2 m-thick upper crust characterised by a mixture of blocks and slabs with rounded and irregularly shaped lapilli, and interstitial ash (herein termed mingled crust), that overlie the more coherent lava and lava crust zones. The characteristic components of RP8 mingled crust vary laterally but broadly comprise ~5–15 cm, moderately (5–20%) vesicular, blocky, angular to sub-angular clasts (Fig. 7B^{i}, C^{i}), or sub-rounded and irregular clasts (Fig. 7D^{i}), with moderately abundant <1 cm phenocrysts, and minor evidence of block recycling (Fig. 7Bi).

Clasts with irregular margins are generally smaller (fine to medium lapilli) and have fewer phenocrysts, although some large (ca. 10–15 cm) clasts with irregular margins are also present (Fig. 7D^{i}). Groundmass components comprise fine to medium ash (Fig. 7B, C), sparse phenocrysts and phenocryst fragments (Fig. 7C), and areas of coarse ash to very fine lapilli (Fig. 7B). In some cross-sectional cuts, folded and stretched slabs and clasts are clearly visible, along with small pockets of interstitial ash (Fig. 7E, E^{i}).

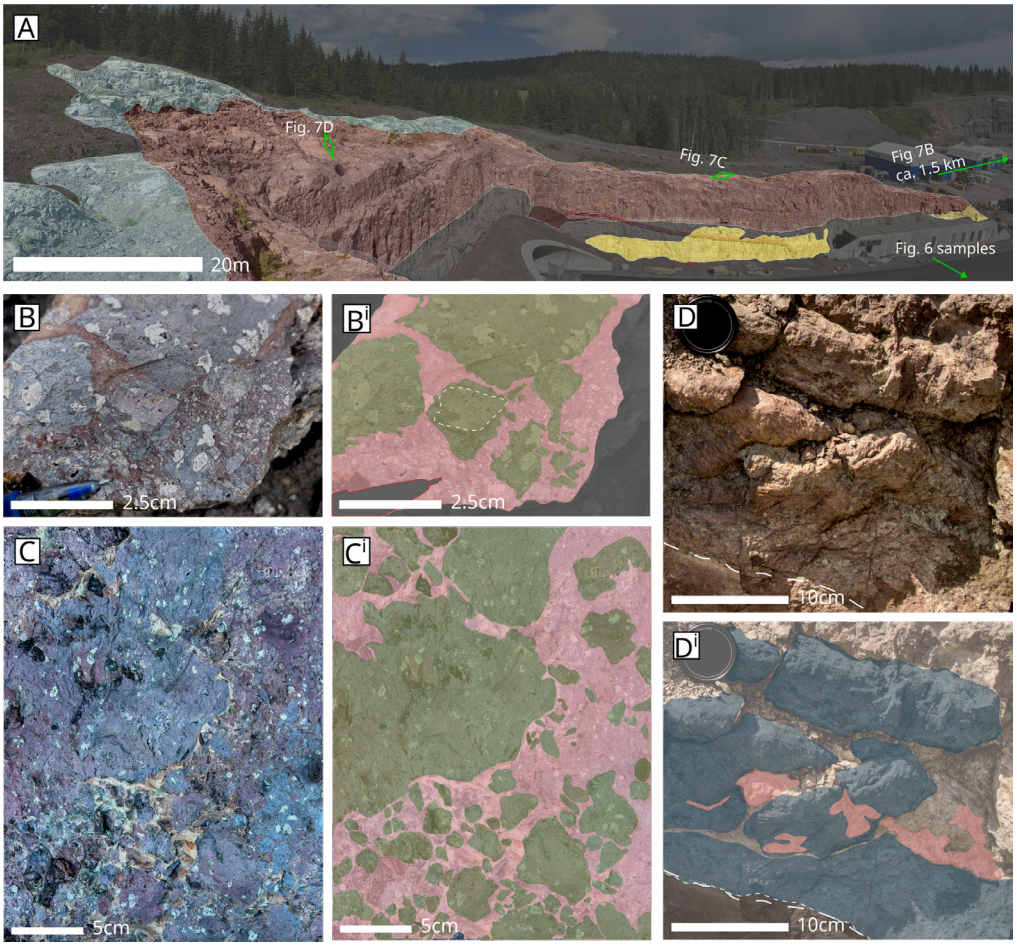

Figure 7. A road-cut outcrop containing RP7, RP8b with mingled crust, and the basal section of RP8d (A) from Avtjerna. Outcrop images (B–D) and simplified interpretations (Bi–Di) of a. Green boxes in outcrop overview image (A) indicate locations where B–D are found. Pink polygons in B^{i}–D^{i} represent interstitial ash (<2 mm size) and fine lapilli (2–4 mm size) components, and some areas of agglomerated fine particles in Di. Mingled crust in B and C contains more clasts (green polygons in Bi & C^{i}) with blocky, angular to sub-angular shapes (white dashed outlines in C^{i}), and shows minor evidence for recycling of blocky clasts (white dashed outline in B^{i}). Comparatively, mingled crust in D and E has a higher abundance of clasts with irregular to amoeboid-shaped forms (green polygons in D^{i}) or stretched and folded pahoehoe-type slabs (blue polygons in Ei). Outcrop location coordinates are: B) 10.385°E, 59.946°N: C) 10.374°E, 59.952°N; and D) 10.373°E, 59.953°N.

Discussion

Feeder-dike or dissected lava

Poor exposure of deposits, contacts, and relationships to adjacent stratigraphy related to the Mjøsundvika and Ammerud RP units makes confident assessment of an extrusive or intrusive origin based on outcrop examination alone challenging. Previous interpretations of these RP outcrops suggested they were poorly preserved remnants of an RP lava flow (Oftedahl, 1957; Naterstad, 1978), where cross-cutting relationships may have resulted from deposition within a pre-existing erosional scour (e.g., reoccupation of an abandoned channel: Ebinghaus et al., 2014; D. Brown et al., 2024). Alternatively, the occurrence of basalt and RP at the same stratigraphic level could result from faulting, which is evident in Alnsjø (Fig. 1C), in part due to later caldera collapse (Whattam et al., 2024). That notwithstanding, stratigraphic juxtaposition on both sides, no evidence for fault movements, and pyroclastic ash-rich margins all provide a strong argument against faulting as the cause of this arrangement. Furthermore, detailed observation across macro- to micro-scale reveals features such as brecciated host rock, ash-rich margins, and vertical or near-vertical contacts, that are difficult to reconcile with an extrusive origin. Pyroclastic ash-rich zones comprising clasts of both the lava and the underlying or adjacent rock are not characteristic of lava flows. Although lavas may have crustal, basal, or marginal breccias (Sparks et al., 1993; Duraiswami et al., 2008; Óskarsson & Riishuus, 2014; Navarrete et al., 2020) these form through auto-brecciation and largely comprise blocky and angular to irregular and scoriaceous clasts (i.e., a'a type) or tabular to curved slabs (i.e., pahoehoe-type) of the cooled lava. In contrast, feeder-dikes of moderately explosive mafic eruptions display textural zones and gradations from lava or welded lapilli tuff, through ash-rich margins, to brecciated host rocks (e.g., Re et al., 2016) comparable to the Mjøsundvika and Ammerud RP outcrops. Thus, we reinterpret the textural characteristics and outcrop arrangement as evidence of an intrusive origin and infer that this was an eruption-feeding dike (i.e., a fissure-conduit).

Erosion has removed any extrusive products such that conduit-lava connections are not preserved. Therefore, accurately placing these outcrops in the context of an eruption paleo-surface with accuracy is not possible. However, dikes with similar pyroclastic features, brecciated margins, and mingled (i.e., peperitic) zones, clastogenic or welded spatter textures have inferred depths less than 85 m from a paleo-surface (Lefebvre et al., 2012; Geshi & Neri, 2014; Re et al., 2016). Feeder-dikes in East Basalt Ridge (Nevada, USA), for example, are characterised by consistent width and sharp margins at >100 m depth, with sub-vertical and sub-planar margins, splays, increasing width, and brecciation between ~100 and 35 m. At depths shallower than 25 m substantial widening (margins at ~45 degrees) takes place (Keating et al., 2008). At shallow depths (<35–40 m) the transition from dike to wall-rock passes from massive basalt, through a breccia of co-mingled basalt and wall rock and altered wall-rock (a tuff vitrophyre in this instance), into unaltered wall-rock (Keating et al., 2008). With the exception of altered wall-rock (vitrophyre development), the lateral textural gradation observed in Mjøsundvika is comparable to the feeder dikes reported by Keating et al. (2008). Consequently, based on significant width (~40 – <100 m), high degree of mingling and breccia development, and steep to sub-vertical margins, we infer that the Mjøsundvika exposure represents a stratigraphic depth of 40–60 m below the eruption paleo-surface.

Explosivity in RP eruptions

In heavily dissected or eroded volcanic provinces, demonstrating a specific eruptive style for the preserved volcanic products can be challenging (Geshi et al., 2010; Carracedo-Sánchez et al., 2017). Furthermore, effusive to explosive transitions are far less documented than the inverse, though not

unheard of (e.g., Neal et al., 2019; Thivet et al., 2020). Whilst RP lava textures in the Oslo Rift have historically been interpreted as indicative of effusive eruptions, the Mjøsundvika and Avtjerna outcrops highlight the development of explosive activity in vent-proximal localities and late to waning stages of eruptive periods. A combination of effusive and explosive eruption is supported by observations from drillcores from the Krokskogen region (Dalslåen et al., 2024; Svensen et al., 2024). These studies emphasize a common textural progression, comprising vesicular basal zones, dense cores, and variably brecciated lava crusts with mingled or overlying pyroclastic components. Similar variability is also observed in flood basalt provinces (e.g., Brown et al., 2014; Óskarsson & Riishuus, 2014) and basaltic feeder systems (e.g., Lefebvre et al., 2012; Re et al., 2016). At Avtjerna, deposits are interpreted as two distinct but related depositional settings: a vent-proximal spatter cone (RP7; Fig. 6) and a mingled lava-crust (RP8; Fig. 7). These are the plausible surficial products of the features observed in the Mjøsundvika and Ammerud outcrops. Welding, clast deformation, and a high proportion of sub-rounded to irregular and fluidal lapilli and ash in the RP7 spatter (Fig. 6B, C, G, H) indicates moderate fragmentation and deposition as hot, ductile pyroclasts. In addition, the highly variable vesicle abundance and degree of flattening suggests a range of clast formation histories prior to final assemblage. Boundaries in RP8 between dense lava, brecciated crust, and mingled zones appear to be gradational, implying that these do not represent distinct eruptive deposits but are cognate to the lava crust. A'a (including platy-, cauliflower, and rubbly-a'a varieties) and rubbly-pahoehoe lava flows are characterised by variably brecciated flow crusts (Duraiswami et al., 2008; Murcia et al., 2014) which likely generates a large proportion of the clasts in the mingled zone. However, the moderately abundant clasts with irregular to amoeboid forms (Fig. 7C), and an interstitial ash to fine to very-fine lapilli components (Fig. 7B, C) are not typically associated with auto-brecciated lava crusts, which commonly consists of angular to sub-angular fragments (e.g., Duraiswami et al., 2014; Óskarsson & Riishuus, 2014). Viewed in combination with the underlying RP7 spatter deposit, partially preserved ash layers overlying RP7 and RP8, minor ash-ingestion in the RP8 pahoehoe crust (Fig. 7D), and the RP fissure-conduit in Alnsjø, there is strong evidence for moderately explosive activity during RP eruptions in the Oslo Rift.

However, RP lavas are intermediate in composition (~55% SiO_2), are thought to have been high in dissolved gases, and erupted at high temperatures (ca. 1,050–1,100°C) with inferred volcanological behaviour similar to Hawaiian basalts (Larsen et al., 2008). That notwithstanding, the actual rheological behaviour of a magma is far more complex than its geochemical composition, and eruption temperatures or dissolved gas content may change during an eruption. Abundant, large phenocrysts, for example, can impart a higher relative viscosity to the magma (Caricchi et al., 2007; Ishibashi, 2009), although the phenocrysts can reduce the relative viscosity at high strain rates (Caricchi et al., 2007). Consistent phenocryst orientations (expected from high strain rate: Caricchi et al., 2007) are only observed in individual clasts of the core zone (Fig. 4A), suggesting that high strain rates occurred either at depth or earlier in the eruption, with these clasts later incorporated through fragmentation or recycling. Vent localisation, cone building, and plug formation (Re et al., 2016; Thivet et al., 2020; Schipper et al., 2021), compositional or textural (e.g., syn-eruptive vesicle or microlite growth) variations (Lipman et al., 1985; Pompilio et al., 2017; Edwards et al., 2018), or changes in conduit geometry (Keating et al., 2008; Lefebvre et al., 2012; Geshi & Oikawa, 2014) can also instigate transitions in eruption style. Locally, failure (i.e., brecciation) of wall-rock will generate energetic strain waves which has the potential to promote periods of explosive activity (Benson et al., 2012). Although surficial aspects (e.g., cone building) and properties such as ascent rate are unknown in the Mjøsundvika and Ammerud fissure-conduits, the abundant vesicles and microlites in the dike core (Fig. 4A[2] & 5D, F), and restricted areal coverage of the RP outcrops suggest that an increase in relative viscosity and vent localisation (further evidenced by spatter deposits at Avtjerna) may have driven a change from effusive to explosive activity.

Age data from Corfu & Larsen (2020) indicate that RP7 and RP8 lavas are significantly younger (ca. 285 Ma) than the onset of RP volcanism at ca. 300 Ma, and closer in time to RP13 (with RP11 dated at ca. 280 Ma) than the earliest RP lavas. Earlier RP lavas may well have erupted in a purely effusive manner, as previously suggested (e.g., Larsen et al., 2008), Later eruptions seem to have become more complex due to changes in the magmatic plumbing system (e.g., ascent rates or depth), variable magma properties (e.g., storage temperature, volatile content, or micro-phenocryst abundance), or fissure geometries. However, deep fragmentation and subsequent intense shallow sintering (cryptic fragmentation: e.g., Wadsworth et al., 2020, 2022; Foster et al., 2024) has been shown as a key mechanism in effusive eruptions, eruption transitions at silicic volcanic centres. Observation of similar textures in basaltic phreatomagmatic and andesitic dome-forming eruptions also indicate this process is not limited to silicic compositions (Wadsworth et al., 2020).

Emplacement model

Textures observed in the Mjøsundvika outcrop and in the associated hand-samples and thin-sections mirror those documented in feeder systems of monogenetic basaltic volcanoes (Re et al., 2016). The textures suggest emplacement comprising at least three distinct stages (Fig. 8). However, similar to aggradation in pyroclastic density currents (e.g., Branney & Kokelaar, 1992), the textures in a magmatic conduit will represent aggradation over the course of an eruption that might continue for months or years (Valentine et al., 2006; Keating et al., 2008; White et al., 2009). Therefore, whilst the Mjøsundvika outcrop represents the final phase of activity, the observed textures should be viewed as a composite record, with some features (such as brecciation) having developed during earlier eruption phases. Differences between the margin zones at Mjøsundvika and Ammerud are therefore viewed as recording variable development, either temporally or spatially. Shallow feeder dikes (i.e., fissure-conduits) commonly have contrasting margins: one sharp margin in contact with relatively homogeneous lava, and the other showing widening, pyroclastic textures, zones with pepperite, and abundant host-rock fragments (Re et al., 2016). Given that we only observe one margin in Ammerud, the narrower, sharper margin between RP and sandstone in Ammerud could simply represent this variability. Nevertheless, both margins in the Mjøsundvika outcrops are characterised by well-developed pyroclastic zones, showing heterogeneous and peperitic textures (Figs. 3 & 4B, C) at approximately the same stratigraphic level as the Ammerud outcrop. Vent localisation, observed in Icelandic (Hjartardóttir et al., 2016) and Hawaiian (Neal et al., 2019) eruptions, can explain temporal variability, whereby some portions of a fissure-conduit are active during the early effusive phase of an eruption (i.e., the Ammerud outcrops) but are inactive during later phases (i.e., explosive pulses recorded in the Mjøsundvika outcrops). However, fissure conduits are not spatially consistent and sites of fragmentation or even diatreme formation (i.e., phreatomagmatic sites) may occur sporadically along a fissure (Re et al., 2016). These variations are possibly related to host-rock variability (e.g., mechanically weak zones) or interaction with spatially restricted water sources (e.g., streams, small lakes, or water-filled fractures). In either case, early eruptive activity from the fissure-conduits was apparently characterised by effusive behaviour (Fig. 8A) with limited to no fragmentation and very-coarse to no wall-rock brecciation. Later explosive activity may have occurred consistently along the length of the fissure or may have been spatially confined.

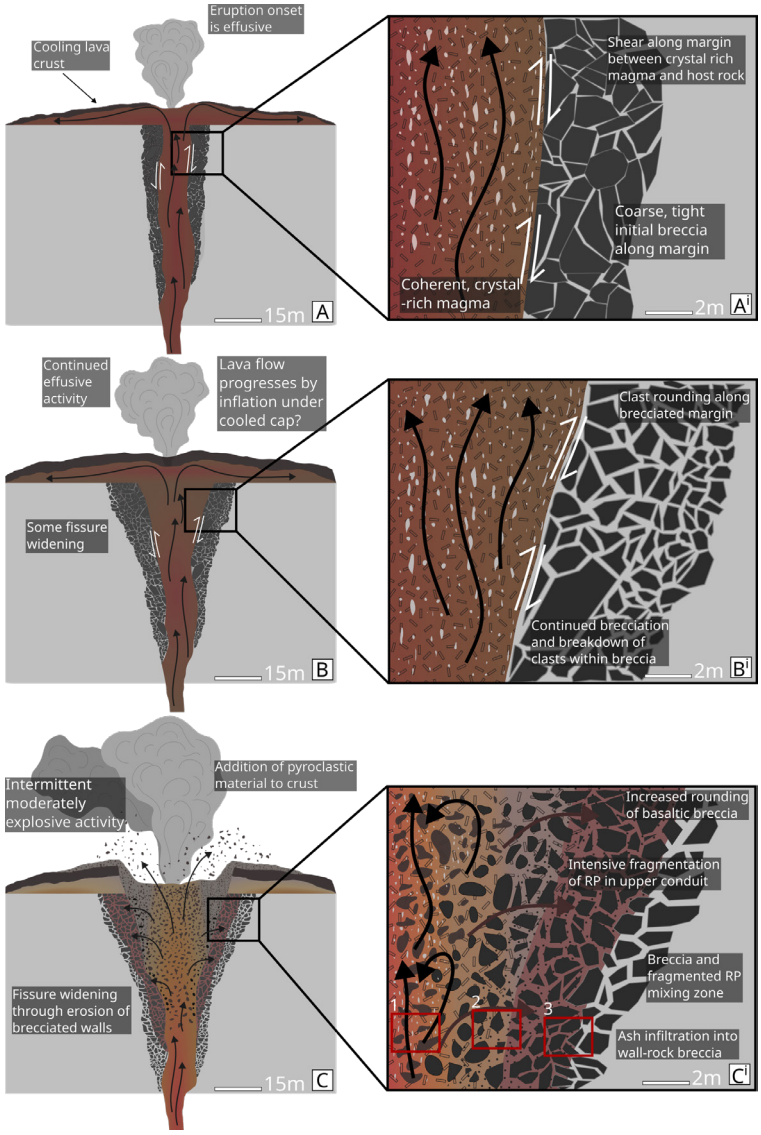

Figure 8. (over-page) Schematic models illustrating proposed dike structure and emplacement mechanisms based on observed textures. A, B, and C are not intended to represent specific time-steps within an eruptive episode (i.e., they are dimensionless). Ai, Bi, and Ci are detailed representations approximating the Mjøsundvika outcrop shown in Fig. 2A. Red boxes in Ci indicate approximate locations of samples in Figs. 4 & 5: Box 1 = Figs. 4A, A1, A2 & 5C–F. Box 2 = Figs. 4B & 5A. Box 3 = Figs. 4C & 5B.

Brecciation and subsequent erosion of the wall-rock facilitated substantial widening (Fig. 8B) of the fissure-conduit (e.g., Geshi & Oikawa, 2014), although brecciation evidently occurred before explosive activity began. If brecciation was driven by shear along the margin in the presence of ash, the expected textural characteristics would include vitrophyre development (i.e., shear densification and welding), clast deformation and alignment, and banding (e.g., Unwin et al., 2023). In addition, brecciation is unlikely to have been driven by the ash-producing fragmentation. Clast shapes (irregular and amoeboidal), subtle flow structures in the core zone (minor phenocryst alignment, elongated and aligned vesicles, minor fiamme), and limited ash volumes (relative to the overall conduit volume) indicate a generally weak and hot fragmentation style (e.g., Lefebvre et al., 2012). Furthermore, the absence of angular lapilli with quench margins suggests that interaction with water (i.e., phreato-magmatism) did not occur (Zimanowski et al., 2015). Hence, fragmentation energy was likely inadequate to drive significant brecciation. Instead, we infer that dike-parallel shear stresses (Delaney & Pollard,

1981; Dering et al., 2019), possibly coincident with hydraulic fracture (i.e., expansion of pore fluids: Delaney & Pollard, 1981; Lefebvre et al., 2012), caused wall-rock brecciation during earlier effusive phases. Prior brecciation would have aided inclusion of small basaltic clasts into the ash-rich zone (Fig. 8Ci), with fragmentation energy only required for disaggregation and incorporation.

Variations in the colour, vesicularity, and crystallinity of the components in the core zone suggest that individual clasts experienced different eruption histories prior to becoming agglomerated and sintered together in the final deposit (Schipper et al., 2021; Marshall et al., 2022). Exsolution of volatiles into a separate phase (i.e., vesicles) will lead to increased viscosity of the remaining melt and can promote sintering (Shields et al., 2016), whilst increasing micro-crystallinity enhances the rheological strength (Lipman et al., 1985). Coupling of vent localisation, changes in magmatic characteristics, decreased ascent rates, and possibly sintering or plug formation may therefore have contributed to a shift toward pulsed explosive activity in the late stage of the RP eruption.

Conclusions

Ideas concerning the characteristic eruptive styles of major volcanic phases in the Oslo Rift have been in need of supporting evidence. In previous studies, the RP unit described here was interpreted as a partially preserved lava flow. However, the stratigraphic juxtaposition of units, pyroclastic textures in the RP, ash-rich marginal zones, and substantial brecciation of wall rocks strongly indicate that the RP is an intrusive unit (i.e., a dike). Thus, the RP outcrop presented here constitutes the first direct evidence of a shallow fissure-conduit and fissure-fed RP eruption in the Oslo Rift. The detailed studies of textures in outcrop, hand-sample, and thin-section provide evidence that the RP eruptions were more complex than generally thought, with mildly to moderately explosive phases likely occurring during late or waning stages of eruptions. This interpretation is supported by the occurrence of complex flow tops in earlier RP eruptions, where ash and lapilli pyroclasts are mingled with larger lava fragments of the flow crust.

Acknowledgements. We thank Statens Vegvesen and Terje Kirkeby for providing access to outcrops within road construction areas in Sollihøgda. We also thank Sverre Planke for his assistance accessing these sites, and drillcore related to prior geotechnical assessments. D. A. Jerram is partly funded through the Research Council of Norway's 'Beyond Elasticity' project (grant 334654) at the NJORD Centre, UIO. J. W. would like to thank Scott Bryan for his insightful thoughts on shallow welded dikes in other magmatic provinces. The authors would also like to thank an anonymous reviewer and the journal editor Espen Torgersen for thoughtful input that improved the quality of the manuscript.

References

Aguirre-Díaz, G.J. & Labarthe-Hernández, G. 2003: Fissure ignimbrites: Fissure-source origin for voluminous ignimbrites of the Sierra Madre Occidental and its relationship with Basin and Range faulting. *Geology 31*. https://doi.org/10.1130/G19665.1

Benson, P.M., Heap, M.J., Lavallée, Y., Flaws, A., Hess, K.-U., Selvadurai, A.P.S., Dingwell, D.B. & Schillinger, B. 2012: Laboratory simulations of tensile fracture development in a volcanic conduit via cyclic magma pressurisation. *Earth and Planetary Science Letters 349–350*, 231–239. https://doi.org/10.1016/j.epsl.2012.07.003

Branney, M.J., Bonnichsen, B., Andrews, G.D.M., Ellis, B., Barry, T. L. & McCurry, M. 2008: "Snake River (SR)-type" volcanism at the Yellowstone hotspot track: distinctive products from unusual, high-temperature silicic super-eruptions. *Bulletin of Volcanology 70*. https://doi.org/10.1007/s00445-007-0140-7

Branney, M.J. & Kokelaar, P. 1992: A reappraisal of ignimbrite emplacement: progressive aggradation and changes from particulate to non-particulate flow during emplacement of high-grade ignimbrite. *Bulletin of Volcanology 54*. https://doi.org/10.1007/BF00301396

Branney, M.J. & Kokelaar, P. 2002: *Pyroclastic Density Currents and the Sedimentation of Ignimbrites*. Geological Society of London. https://doi.org/10.1144/GSL.MEM.2003.027

Brown, D., Quirie, A., Reynolds, P. & Drake, S. 2024: "Hot and sticky" and "cold and damp" pyroclastic eruptions, and their relationship with topography: valley- and lake-filling ignimbrites, Ardnamurchan, NW Scotland. *Volcanica 7*. https://doi.org/10.30909/vol.07.02.503524

Brown, R.J., Blake, S., Thordarson, T. & Self, S. 2014: Pyroclastic edifices record vigorous lava fountains during the emplacement of a flood basalt flow field, Roza Member, Columbia River Basalt Province, USA. *GSA Bulletin 126*. https://doi.org/10.1130/B30857.1

Brown, R.J. & Branney, M.J. 2004: Bypassing and diachronous deposition from density currents: Evidence from a giant regressive bed form in the Poris ignimbrite, Tenerife, Canary Islands. *Geology 32*. https://doi.org/10.1130/G20188.1

Brown, R.J. & Branney, M.J. 2013: Internal flow variations and diachronous sedimentation within extensive, sustained, density-stratified pyroclastic density currents flowing down gentle slopes, as revealed by the internal architectures of ignimbrites on Tenerife. *Bulletin of Volcanology 75*. https://doi.org/10.1007/s00445-013-0727-0

Bryan, S.E., Ewart, A., Stephens, C.J., Parianos, J. & Downes, P.J. 2000: The Whitsunday Volcanic Province, Central Queensland, Australia: lithological and stratigraphic investigations of a silicic-dominated large igneous province. *Journal of Volcanology and Geothermal Research 99,* 55–78. https://doi.org/10.1016/S0377-0273(00)00157-8

Burchardt, S. 2008: New insights into the mechanics of sill emplacement provided by field observations of the Njardvik Sill, Northeast Iceland. *Journal of Volcanology and Geothermal Research 173*. https://doi.org/10.1016/j.jvolgeores.2008.02.009

Caricchi, L., Burlini, L., Ulmer, P., Gerya, T., Vassalli, M. & Papale, P. 2007: Non-Newtonian rheology of crystal-bearing magmas and implications for magma ascent dynamics. *Earth and Planetary Science Letters 264*, 402–419. https://doi.org/10.1016/j.epsl.2007.09.032

Carracedo-Sánchez, M., Sarrionandia, F., Ábalos, B., Errandonea-Martin, J. & Gil Ibarguchi, J.I. 2017: Intra-cone plumbing system and eruptive dynamics of small-volume basaltic volcanoes: A case study in the Calatrava Volcanic Field. *Journal of Volcanology and Geothermal Research 348*, 82–95. https://doi.org/10.1016/j.jvolgeores.2017.10.014

Corfu, F. & Larsen, B. 2020: U-Pb systematics in volcanic and plutonic rocks of the Krokskogen area: Resolving a 40 million years long evolution in the Oslo Rift. *Lithos 376–377*, 105755. https://doi.org/10.1016/j.lithos.2020.105755

Dalslåen, B.H., Planke, S. & Svensen, H.H. 2024: Conquering the sub-surface: Taking on the Oslo Rift lava pile and infrastructure development. In Regnéll, C., Zack, T., Holme, K. & Andersson, J. (eds.): *36th nordic geological winter meeting, Göteborg, January 10–12 2024, Abstract volume*. Geologiska Föreningen Specialpublikation 5, p. 99. https://geologiskaforeningen.se/wp-content/uploads/2024/04/GF_SP5_2024_abstract-volume.pdf

Delaney, P.T. & Pollard, D.D. 1981: Deformation of host rocks and flow of magma during growth of minette dikes and breccia-bearing intrusions near Ship Rock, New Mexico. *U.S. G.P.O. 1202*, 61 pp. https://doi.org/10.3133/pp1202

Dering, G.M., Micklethwaite, S., Cruden, A.R., Barnes, S.J. & Fiorentini, M.L. 2019: Evidence for dyke-parallel shear during syn-intrusion fracturing. *Earth and Planetary Science Letters 507*, 119–130. https://doi.org/10.1016/j.epsl.2018.10.024

Díaz-Bravo, B.A. & Morán-Zenteno, D.J. 2011: The exhumed Eocene Sultepec-Goleta Volcanic Center of southern Mexico: record of partial collapse and ignimbritic volcanism fed by wide pyroclastic dike complexes. *Bulletin of Volcanology 73*. https://doi.org/10.1007/s00445-011-0460-5

Duraiswami, R.A., Bondre, N.R. & Managave, S. 2008: Morphology of rubbly pahoehoe (simple) flows from the Deccan Volcanic Province: Implications for style of emplacement. *Journal of Volcanology and Geothermal Research 177*. https://doi.org/10.1016/j.jvolgeores.2008.01.048

Duraiswami, R.A., Gadpallu, P., Shaikh, T.N. & Cardin, N. 2014: Pahoehoe–a'a transitions in the lava flow fields of the western Deccan Traps, India-implications for emplacement dynamics, flood basalt architecture and volcanic stratigraphy. *Journal of Asian Earth Sciences 84*, 146–166. https://doi.org/10.1016/j.jseaes.2013.08.025

Ebinghaus, A., Hartley, A.J., Jolley, D.W., Hole, M. & Millett, J. 2014: Lava–Sediment Interaction and Drainage-System Development In A Large Igneous Province: Columbia River Flood Basalt Province, Washington State, U.S.A. *Journal of Sedimentary Research 84*. https://doi.org/10.2110/jsr.2014.85

Edwards, M.J., Pioli, L., Andronico, D., Scollo, S., Ferrari, F. & Cristaldi, A. 2018: Shallow factors controlling the explosivity of basaltic magmas: The 17–25 May 2016 eruption of Etna Volcano (Italy). *Journal of Volcanology and Geothermal Research 357*, 425–436. https://doi.org/10.1016/j.jvolgeores.2018.05.015

Foster, A., Wadsworth, F.B., Tuffen, H., Unwin, H.E. & Humphreys, M.C.S. 2024: Evidence for the formation of silicic lava by pyroclast sintering. *Nature Communications 15*, 5347. https://doi.org/10.1038/s41467-024-49601-6

Galindo, I. & Gudmundsson, A. 2012: Basaltic feeder dykes in rift zones: geometry, emplacement, and effusion rates. *Natural Hazards and Earth System Sciences 12*, 3683–3700. https://doi.org/10.5194/nhess-12-3683-2012

Galland, O., Planke, S., Neumann, E.-R. & Malthe-Sørenssen, A. 2009: Experimental modelling of shallow magma emplacement: Application to saucer-shaped intrusions. *Earth and Planetary Science Letters 277*. https://doi.org/10.1016/j.epsl.2008.11.003

Galland, O., Spacapan, J.B., Rabbel, O., Mair, K., Soto, F.G., Eiken, T., Schiuma, M. & Leanza, H.A. 2019: Structure, emplacement mechanism and magma-flow significance of igneous fingers – Implications for sill emplacement in sedimentary basins. *Journal of Structural Geology 124*, 120–135. https://doi.org/10.1016/j.jsg.2019.04.013

Geshi, N., Kusumoto, S. & Gudmundsson, A. 2010: Geometric difference between non-feeder and feeder dikes. *Geology 38*, 195–198. https://doi.org/10.1130/G30350.1

Geshi, N. & Neri, M. 2014: Dynamic feeder dyke systems in basaltic volcanoes: the exceptional example of the 1809 Etna eruption (Italy). *Frontiers in Earth Science 2*. https://doi.org/10.3389/feart.2014.00013

Geshi, N. & Oikawa, T. 2014: The spectrum of basaltic feeder systems from effusive lava eruption to explosive eruption at Miyakejima volcano, Japan. *Bulletin of Volcanology 76*, 797. https://doi.org/10.1007/s00445-014-0797-7

Giachetti, T., Trafton, K.R., Wiejaczka, J., Gardner, J.E., Watkins, J.M., Shea, T. & Wright, H.M.N. 2021: The products of primary magma fragmentation finally revealed by pumice agglomerates. *Geology 49*, 1307–1311. https://doi.org/10.1130/G48902.1

Heiken, G., Wohletz, K. & Eichelberger, J. 1988: Fracture fillings and intrusive pyroclasts, Inyo Domes, California. *Journal of Geophysical Research: Solid Earth 93*, 4335–4350. https://doi.org/10.1029/JB093iB05p04335

Hjartardóttir, Á.R., Einarsson, P., Gudmundsson, M.T. & Högnadóttir, T. 2016: Fracture movements and graben subsidence during the 2014 Bárðarbunga dike intrusion in Iceland. *Journal of Volcanology and Geothermal Research 310*, 242–252. https://doi.org/10.1016/j.jvolgeores.2015.12.002

Holtedahl, O. 1943: Some structural features of the district near Oslo. *In Studies on the igneous rock complex of the Oslo region 1*, Skrifter Norske Videnskaps Akademi I Oslo, 98 pp.

Ishibashi, H. 2009: Non-Newtonian behavior of plagioclase-bearing basaltic magma: Subliquidus viscosity measurement of the 1707 basalt of Fuji volcano, Japan. *Journal of Volcanology and Geothermal Research 181*, 78–88. https://doi.org/10.1016/j.jvolgeores.2009.01.004

Kano, K. 2002: Middle Miocene volcaniclastic dikes at Kukedo, Shimane Peninsula, SW Japan: fluidization of volcaniclastic beds by emplacement of syn-volcanic andesitic dikes. *Journal of Volcanology and Geothermal Research 114*, 81–94. https://doi.org/10.1016/S0377-0273(01)00283-9

Keating, G.N., Valentine, G.A., Krier, D.J. & Perry, F.V. 2008: Shallow plumbing systems for small-volume basaltic volcanoes. *Bulletin of Volcanology 70*. https://doi.org/10.1007/s00445-007-0154-1

Larsen, B., Olaussen, S., Sundvoll, B. & Heeremans, M. 2008: The Permo-Carboniferous Oslo Rift through six stages and 65 million years. *Episodes 31*. https://doi.org/10.18814/epiiugs/2008/v31i1/008

Lefebvre, N.S., White, J.D.L. & Kjarsgaard, B.A. 2012: Spatter-dike reveals subterranean magma diversions: Consequences for small multivent basaltic eruptions. *Geology 40*. https://doi.org/10.1130/G32794.1

Lipman, P.W., Banks, N.G. & Rhodes, J.M. 1985: Degassing-induced crystallization of basaltic magma and effects on lava rheology. *Nature 317*, 604–607. https://doi.org/10.1038/317604a0

Manville, V., Németh, K. & Kano, K. 2009: Source to sink: A review of three decades of progress in the understanding of volcaniclastic processes, deposits, and hazards. *Sedimentary Geology 220*. https://doi.org/10.1016/j.sedgeo.2009.04.022

Marshall, A.A., Manga, M., Brand, B.D. & Andrews, B.J. 2022: Autobrecciation and fusing of mafic magma preceding explosive eruptions. *Geology 50*, 1177–1181. https://doi.org/10.1130/G50180.1

Murcia, H., Németh, K., Moufti, M.R., Lindsay, J.M., El-Masry, N., Cronin, S.J., Qaddah, A. & Smith, I.E.M. 2014: Late Holocene lava flow morphotypes of northern Harrat Rahat, Kingdom of Saudi Arabia: Implications for the description of continental lava fields. *Journal of Asian Earth Sciences 84*, 131–145. https://doi.org/10.1016/j.jseaes.2013.10.002

Naterstad, J. 1978: Excursion 2. Nittedal cauldron (Alnsjøen area). *The Oslo paleorift - A review and guide to excursions*. https://hdl.handle.net/11250/2675052

Navarrete, C., Butler, K.L., Hurley, M. & Márquez, M. 2020: An early Jurassic graben caldera of Chon Aike silicic LIP at the southernmost massif of the world: The Deseado caldera, Patagonia, Argentina. *Journal of South American Earth Sciences 101*, 102626. https://doi.org/10.1016/j.jsames.2020.102626

Navarrete, C., Hurley, M., Butler, K., Liendo, I., Litvak, V. & Folguera, A. 2021: Jurassic volcanism of the Chon Aike Silicic LIP in the northeastern Deseado Massif. *Journal of South American Earth Sciences 107*, 102886. https://doi.org/10.1016/j.jsames.2020.102886

Neal, C.A., Brantley, S.R., Antolik, L., Babb, J.L., Burgess, M., Calles, K., Cappos, M., Chang, J.C., Conway, S., Desmither, L., Dotray, P., Elias, T., Fukunaga, P., Fuke, S., Johanson, I.A., Kamibayashi, K., Kauahikaua, J., Lee, R.L., Pekalib, S., Miklius, A., Million, W., Moniz, C.J., Nadeau, P.A., Okubo,P., Parcheta, C., Patrick, M.R., Shiro, B., Swanson, D.A., Tollett, W., Trusdell, F., Younger, E.F., Zoeller, M.H., Montgomery-Brown, E.K., Anderson, K.R., Poland, M.P., Ball, J.L., Bard, J., Coombs, M., Dietterich, H.R., Kern, C., Thelen, W.A., Cervelli, P.F., Orr, T., Houghton, B.F., Gansecki, C., Hazlett, R., Lundgren, P., Diefenbach, A.K., Lerner, A.H., Waite, G., Kelly, P., Clor, L., Werner, C., Mulliken, K., Fisher, G. & Damby, D. 2019: The 2018 rift eruption and summit collapse of Kīlauea Volcano. *Science 363*, 367–374. https://doi.org/10.1126/science.aav7046

Neumann, E.-R. 2019: Origin and evolution of the early magmatism in the Oslo Rift (Southeast Norway): Evidence from multiple generations of clinopyroxene. *Lithos 340–341*, 139–151. https://doi.org/10.1016/j.lithos.2019.04.025

Neumann, E.-R., Olsen, K.H. & Baldridge, W.S. 2006: Chapter 9 The Oslo rift. In Olsen, K.H. (ed.): *Developments in Geotectonics*, Elsevier 25, pp. 345–373. https://doi.org/10.1016/S0419-0254(06)80017-0

Oftedahl, C. 1957: On Ignimbrite and Related Rocks. *In Studies on the Igneous Rock Complex of the Oslo Region 2*, Skrifter Norske Videnskaps Akademi I Oslo, 98 pp.

Oftedahl, C. 1959: Volcanic sequence and magma formation in the Oslo region. Geologische Rundschau 48. https://doi.org/10.1007/BF01801806

Oftedahl, C. 1978a: Main Geologic Features of the Oslo Graben. *In* Ramberg, I. & Neumann, E.R. (eds.): *Tectonics and Geophysics of Continental Rifts*, NATO Advanced Study Institutes Series 37, pp. 149–165. https://doi.org/10.1007/978-94-009-9806-3_14

Oftedahl, C. 1978b: Cauldrons of the Permian Oslo rift. J*ournal of Volcanology and Geothermal Research 3*. https://doi.org/10.1016/0377-0273(78)90043-4

Olaussen, S., Larsen, B. & Steel, R. 1994: The Upper Carboniferous-Permian Oslo Rift; Basin Fill in Relation to Tectonic Development. *In Pangea: Global Environments and Resources*, Canadian Society of Petroleum Geologists Special Publications 17, pp. 175–197.

Óskarsson, B.V. & Riishuus, M.S. 2014: The mode of emplacement of Neogene flood basalts in eastern Iceland: Facies architecture and structure of simple aphyric basalt groups. *Journal of Volcanology and Geothermal Research 289*, 170–192. https://doi.org/10.1016/j.jvolgeores.2014.11.009

Pompilio, M., Bertagnini, A., Del Carlo, P. & Di Roberto, A. 2017: Magma dynamics within a basaltic conduit revealed by textural and compositional features of erupted ash: the December 2015 Mt. Etna paroxysms. *Scientific Reports 7*, 4805. https://doi.org/10.1038/s41598-017-05065-x

Rämö, O.T., Andersen, T. & Whitehouse, M.J. 2022: Timing and Petrogenesis of the Permo-Carboniferous Larvik Plutonic Complex, Oslo Rift, Norway: New Insights from U–Pb, Lu-Hf, and O Isotopes in Zircon. *Journal of Petrology 63*. https://doi.org/10.1093/petrology/egac116

Re, G., White, J.D.L., Muirhead, J.D. & Ort, M.H. 2016: Subterranean fragmentation of magma during conduit initiation and evolution in the shallow plumbing system of the small-volume Jagged Rocks volcanoes (Hopi Buttes Volcanic Field, Arizona, USA). *Bulletin of Volcanology 78*. https://doi.org/10.1007/s00445-016-1050-3

Ross, P.-S., Ukstins Peate, I., McClintock, M.K., Xu, Y.G., Skilling, I.P., White, J.D.L. & Houghton, B.F. 2005: Mafic volcaniclastic deposits in flood basalt provinces: A review. *Journal of Volcanology and Geothermal Research 145*. https://doi.org/10.1016/j.jvolgeores.2005.02.003

Sæther, E. 1946: The area of sediments and lavas in Nittedal. *In Studies on the igneous rock complex of the Oslo region 1*, Skrifter Norske Videnskaps Akademi I Oslo, 34 pp.

Sæther, E. 1962: General investigation of the igneous rocks in the area north of Oslo. *In Studies on the igneous rock complex of the Oslo region 2*, Skrifter Norske Videnskaps Akademi I Oslo, 184 pp.

Schipper, C.I., Castro, J.M., Kennedy, B.M., Tuffen, H., Whattam, J., Wadsworth, F.B., Paisley, R., Fitzgerald, R.H., Rhodes, E., Schaefer, L.N., Ashwell, P.A., Forte, P., Seropian, G. & Alloway, B.V. 2021: Silicic conduits as supersized tuffisites: Clastogenic influences on shifting eruption styles at Cordón Caulle volcano (Chile). *Bulletin of Volcanology 83*. https://doi.org/10.1007/s00445-020-01432-1

Shields, J.K., Mader, H.M., Caricchi, L., Tuffen, H., Mueller, S., Pistone, M. & Baumgartner, L. 2016: Unravelling textural heterogeneity in obsidian: Shear-induced outgassing in the Rocche Rosse flow. *Journal of Volcanology and Geothermal Research 310*, 137–158. https://doi.org/10.1016/j.jvolgeores.2015.12.003

Sohn, C. & Sohn, Y.K. 2019: Distinguishing between primary and secondary volcaniclastic deposits. *Scientific Reports 9*. https://doi.org/10.1038/s41598-019-48933-4

Sparks, R.S.J., Stasiuk, M.V., Gardeweg, M. & Swanson, D.A. 1993: Welded breccias in andesite lavas. *Journal of the Geological Society 150*, 897–902. https://doi.org/10.1144/gsjgs.150.5.0897

Sundvoll, B. & Larsen, B. 1994: Architecture and early evolution of the Oslo Rift. *Tectonophysics 240*. https://doi.org/10.1016/0040-1951(94)90271-2

Sundvoll, B., Neumann, E.-R., Larsen, B. & Tuen, E. 1990: Age relations among Oslo Rift magmatic rocks: implications for tectonic and magmatic modelling. *Tectonophysics 178*. https://doi.org/10.1016/0040-1951(90)90460-P

Svensen, H.H., Callegaro, S., Kjøll, H.J., Midtkandal, I., Whattam, J., Dalslåen, B.H., Kirkeby, T.R., Neumann, E.-R., Millett, J. & Planke, S. 2024: Rhomb porphyry lavas from the Oslo Rift revisited: New insights from construction-related boreholes and cores. *Abstract Volume 5*, 528.

Thivet, S., Gurioli, L., Di Muro, A., Derrien, A., Ferrazzini, V., Gouhier, M., Coppola, D., Galle, B. & Arellano, S. 2020: Evidences of Plug Pressurization Enhancing Magma Fragmentation During the September 2016 Basaltic Eruption at Piton de la Fournaise (La Réunion Island, France). *Geochemistry, Geophysics, Geosystems 21*, e2019GC008611. https://doi.org/10.1029/2019GC008611

Torsvik, T. H., Smethurst, M.A., Burke, K. & Steinberger, B. 2008: Long term stability in deep mantle structure: Evidence from the ~300 Ma Skagerrak-Centered Large Igneous Province (the SCLIP). *Earth and Planetary Science Letters 267*. https://doi.org/10.1016/j.epsl.2007.12.004

Tuffen, H., Dingwell, D.B. & Pinkerton, H. 2003: Repeated fracture and healing of silicic magma generate flow banding and earthquakes? *Geology 31*, 1089–1092. https://doi.org/10.1130/G19777.1

Tuffen, H., James, M.R., Castro, J.M. & Schipper, C.I. 2013: Exceptional mobility of an advancing rhyolitic obsidian flow at Cordón Caulle volcano in Chile. *Nature Communications 4*. https://doi.org/10.1038/ncomms3709

Unwin, H.E., Tuffen, H., Phillips, E., Wadsworth, F.B. & James, M.R. 2021: Pressure-Driven Opening and Filling of a Volcanic Hydrofracture Recorded by Tuffisite at Húsafell, Iceland: A Potential Seismic Source. *Frontiers in Earth Science 9*, 668058. https://doi.org/10.3389/feart.2021.668058

Unwin, H.E., Tuffen, H., Wadsworth, F.B., Phillips, E.R., James, M.R., Foster, A., Kolzenburg, S., Castro, J.M. & Porritt, L.A. 2023: The exposed Mule Creek vent deposits record the structure of a volcanic conduit during a hybrid explosive–effusive eruption. *Bulletin of Volcanology 85*. https://doi.org/10.1007/s00445-023-01638-z

Valentine, G.A., Perry, F.V., Krier, D., Keating, G.N., Kelley, R.E. & Cogbill, A.H. 2006: Small-volume basaltic volcanoes: Eruptive products and processes, and posteruptive geomorphic evolution in Crater Flat (Pleistocene), southern Nevada. *GSA Bulletin 118*, 1313–1330. https://doi.org/10.1130/B25956.1

Vezzoli, L. & Corazzato, C. 2016: Volcaniclastic dykes tell on fracturing, explosive eruption and lateral collapse at Stromboli volcano (Italy). *Journal of Volcanology and Geothermal Research 318*, 55–72. https://doi.org/10.1016/j.jvolgeores.2016.03.009

Wadsworth, F.B., Llewellin, E.W., Vasseur, J., Gardner, J.E. & Tuffen, H. 2020: Explosive-effusive volcanic eruption transitions caused by sintering. *Science Advances 6*. https://doi.org/10.1126/sciadv.aba7940

Wadsworth, F.B., Llewellin, E., Castro, J., Tuffen, H., Schipper, C., Gardner, J., Vasseur, J., Foster, A., Damby, D., McIntosh, I., Boettcher, S., Unwin, H., Heap, M., Farquharson, J., Dingwell, D., Iacovino, K., Paisley, R., Jones, C. & Whattam, J. 2022: A reappraisal of explosive–effusive silicic eruption dynamics: syn-eruptive assembly of lava from the products of cryptic fragmentation. *Journal of Volcanology and Geothermal Research 432*, 107672. https://doi.org/10.1016/j.jvolgeores.2022.107672

Whattam, J.W., Midtkandal, I., Jerram, D.A., Callegaro, S., Svensen, H.H. 2024: The episodic onset of explosive and silicic-dominated volcanism in a continental rift; insights from the Permian Oslo Rift, Norway. *Volcanica 7*, 925–951. https://doi.org/10.30909/vol.07.02.925951

White, J.D.L., Bryan, S.E., Ross, P.S., Self, S. & Thordarson, T. 2009: Physical volcanology of continental large igneous provinces: update and review. *In* Thordarson, T., Self, S., Larsen, G., Rowland, S.K. & Hoskuldsson, A. (eds.): *Studies in Volcanology: The Legacy of George Walker*, The Geological Society of London on behalf of The International Association of Volcanology and Chemistry of the Earth's Interior, pp. 291–321. https://doi.org/10.1144/IAVCEI002.15

Zimanowski, B., Büttner, R., Dellino, P., White, J.D.L. & Wohletz, K.H. 2015: Magma–Water Interaction and Phreatomagmatic Fragmentation. *In* Sigurdsson, H. (ed.): *The Encyclopedia of Volcanoes (Second Edition)*, Academic Press, pp. 473–484. https://doi.org/10.1016/B978-0-12-385938-9.00026-2